Food Chemistry: X 16 (2022) 100486

Contents lists available at ScienceDirect

Food Chemistry: X

journal homepage: www.sciencedirect.com/journal/food-chemistry-x

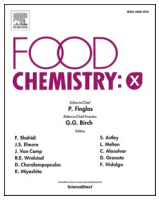

Extraction optimization and characterization of persimmon peel pectin extracted by subcritical water

Yanlong Cui, Shuang Wang, Shuxuan Wang, Siyue Cao, Xin Wang, Xin Lü *

Lab of Bioresources, College of Food Science and Engineering, Northwest A&F University, Yangling 712100, Shaanxi Province, China

ARTICLE INFO

Keywords:
Persimmon peel
Pectin
Subcritical water
Gut microbiota

ABSTRACT

Persimmon peel pectin (PPP) was extracted by subcritical water via the response surface methodology. The optimal crude PPP extraction yield of 7.62 ± 0.7 % was found at 138 °C, 2.84 min, and liquid–solid ratio of 1:10.02. After treatment of deproteinization and decolorization with papain and hydrogen peroxide, 83.19 % of protein and 78.56 % of the colour in crude PPP were removed, respectively. PPP owned the M_w of 21.79 kDa and its uronic acids content was 64.03 %. PPP was further affirmed by fourier transform infrared, X-ray diffractometer and ^{1}H NMR analysis. Moreover, the degradation temperature (228.05 ℃) of PPP was verified via differential scanning calorimetry. Then, the IC_{50} of PPP to ABTS•+ was 9.8 times that of commercial citrus pectin. Moreover, PPP could change microbial communities and selectively enrich *Bacteroides*, *Cetobacterium*, *Erysipelatoclostridium*, *Parabacteroides* and *Phocaeicola sartorii*. This study demonstrated that subcritical water was practicable for extraction of persimmon peel pectin.

1. Introduction

Persimmon (*Diospyros kaki* Thunb.), ready-to-eat fruit, is delicious and popular in East Asian countries. China's annual persimmon output ranks first around the world and Shaanxi province is one of the main persimmon producing areas in China (Jiang, Xu, Li, Li, & Huang, 2020). Persimmon peel results as a key byproduct during the production of dried persimmon (Hamauzu & Suwannachot, 2019). Persimmon peel is a good source of colour, polyphenols and tannin (Smrke, Persic, Veberic, Sircelj, & Jakopic, 2019). What's more, persimmon peel may be a latent new pectin precursor because of its high concentration pectin (Yoo & Shin, 2020). Pectin is a group of complex polysaccharides with polycationic nature and mainly existed in cell-walls of terrestrial plants. Pectin is consisted of the main chain of α-1,4-linked D-galacturonic acid (partly presence of methyl-esterified or acetylated regions) and side chains coupled with a large of neutral sugars (such as arabinose, rhamnose, galactose and xylose) (Mohnen, 2008). Until now, only citric acid solution and *Aspergillus terreus* were used for extraction of persimmon peel pectin (PPP) (Jiang et al., 2020; Liu, Yao, & Fan, 2015; Munoz-Almagro, Vendrell-Calatayud, Mendez-Albinana, Moreno, Cano, & Villamiel, 2021). Therefore, it is meaningful to exploit new extraction methods of PPP to enrich its research.

Subcritical water (SCW) is simple, acid-free, and enzyme-free extraction method compared with other extraction methods (acid and enzyme). SCW could suppose water to liquid state under high temperature (100–374 ℃) and liberal high pressure (0.1–22.1 MPa) along with the changes in dielectric constant and ionic products (Das & Arora, 2021). It has been used to pectin extraction from agricultural by-products in a laboratory scale, such as citrus peel (Ueno, Tanaka, Hosino, Sasaki, & Goto, 2008) and jackfruit peel (Li, Fan, Wu, Jiang, & Shi, 2019). Pectin extracted by SCW tended to have characteristics of low molecular weight (Mw), more hairy regions (also named the rhamnogalacturonan-I (RG-I) regions) and side chains (Basak & Annapure, 2022). However, little information is available regarding PPP extracted by SCW. The structural and functional characteristics of PPP extracted by subcritical water are still poorly known.

Gut microbiota is a complex microbial community, which plays a considerable role in human health (Si-Yuan et al., 2021). Diet can

Abbreviations: PPP, Persimmon peel pectin; CPPP, Crude persimmon peel pectin; CCP, Commercial citrus pectin; SCW, Subcritical water; GAE, Gallic acid equivalents; DE, Degree of esterification; TPC, Total phenolic content; GC, Gas chromatography; HPGPC, High performance gel permeation chromatography; M_w, Molecular weight; XRD, X-ray diffraction; NMR, Nuclear magnetic resonance; DSC, Differential scanning calorimetric; PLS-DA, Partial least squares discriminant analysis; LefSe, Linear discriminant analysis coupled with effect size.

* Corresponding author.
E-mail address: xinlu@nwsuaf.edu.cn (X. Lü).

https://doi.org/10.1016/j.fochx.2022.100486
Received 12 May 2022; Received in revised form 18 October 2022; Accepted 19 October 2022
Available online 20 October 2022

significantly impact microbial communities and metabolism, such as polysaccharides (Chun et al., 2018). It was reported Ganoderma lucidum polysaccharides improved the microbial diversity and ratio of Bacteroides/Firmicutes (Khan et al., 2019). Dietary polysaccharide can also regulate microbial communities and selectively enrich some specific microorganisms, such as *Bacteroides*, *Parabacteroides* (Zhenjun et al., 2022) and *Parabacteroides goldsteinii* (Wu et al., 2019). However, the effect of dietary PPP on gut microbiota was also uncertain.

The overall focus of this study was to study the possibility of using subcritical water in pectin extraction from persimmon peel. This present study aimed to find out the optimal extraction yield of crude persimmon peel pectin (PPP) by subcritical water. Then the crude PPP was applied to the deproteinization and decolorization. Subsequently, the physicochemical properties (chemical composition, monosaccharide composition, molecular weight, and degree of esterification), structural properties (scanning spectra of UV, FTIR, and ^{1}H NMR as well as micromorphology), functional properties (thermal stability, in vitro antioxidant activity), and effects on gut microbiota communities in mice of obtained PPP were also investigated. Our present results would provide a theoretical basis for the potential application of PPP in food or pharmaceutical industry.

2. Material and methods

2.1. Experimental materials and reagents

Persimmon peel was the by-product of dried persimmon processing and collected from four local factories located in Fuping county of Shanxi Province (China). Commercial citrus pectin (CCP) and Folin-Ciocalteu reagent (Cat: F8060) were got from Solarbio Beijing Science & Technology Co., Ltd (CAS: 9000-69-5). DPPH•, ABTS•+, rhamnose (Rha), fucose (Fuc), arabinose (Ara), xylose (Xyl), mannose (Man), glucose (Glu), galactose (Gal), glucuronic acid (GluA), galacturonic acid (GalA) used in this study were got from Sigma chemical Co. (USA). The remaining reagents used in this work were of analytical grade.

2.2. Extraction of persimmon peel pectin by subcritical water

2.2.1. Extraction of CPPP

The dried persimmon peel was crushed by ultra-fine crusher, passed through a 100 mesh sieve, and dried at 60 ℃ for 12 h. Then crude persimmon peel pectin (CPPP) was extracted by subcritical water in a high temperature and high pressure reactor with some modifications (Wang & Lu, 2014). In summary, the mixture of persimmon peel power (adjust the dosage according to ratio of S:W) and distilled water (fixed at 200 mL) was added to working reactor with the total volume of 500 mL, then the reactor was sealed, exhausted with N_2 for 5 min and heated with an electric heating furnace to the set temperature, followed by keeping this temperature to set extraction time. The reactor system was promptly cooled to 55 ℃ with an inside condensation flue loaded with tap water when the extraction time reached to the set value.

The reaction solution was centrifuged at 6000 r/min and 4℃ for 15 min after natural cooling to room temperature. Then the supernatant was filtrated with circulating water vacuum pump, and precipitated overnight with industrial ethanol (95 %) at the ratio of 1:5. The alcohol precipitation solution was centrifuged (6000 r/min, 4℃, 15 min). Then the precipitation was washed with 100 mL anhydrous ethanol and centrifuged (6000 r/min, 4℃, 15 min) for 3 times. After alcohol washing, the solid was freeze-dried and crushed through a 100 mesh sieve. The crude persimmon peel pectin (CPPP) was collected. The CPPP yield was calculated according to equation (1) as follow:

$$\text{CPPP yield}(\%) = \frac{\text{Crude persimmon peel pectin (g)}}{\text{Persimmon peel (g)}} \times 100\% \quad (1)$$

2.2.2. Single factor experimental design

The single factor experimental design was used to analyze the extraction variables including extraction temperature (120, 130, 140, 150, 160, 170 °C), extraction time (1, 3, 5, 7 and 10 min), ratio of solid–liquid (1:5, 1:10, 1:15, 1:20, 1:25 and 1:30 g/mL) and stirring rate (0, 60, 120, 180, 240 and 360 r/min). In this part, the extraction yield of CPPP was a single dependent variable.

2.2.3. BBD experimental design

Response surface methodology (RSM) was used to get the optimal extraction yield of CPPP (%). Subsequently, 17-run experiments were performed via box–behnken design (BBD) based on three variables in three levels (Supplementary Table 1). Then the regression analysis as well as model optimization in this part was conducted in Design Expert 8.06.

2.2.4. Deproteinization and decolorization of CPPP

Papain (BioReagent, P3250, 3, 500 U/mg) was applied to deproteinization of CPPP. Briefly, 0.2 mL papain (10 mg/mL) was mixed with 10 mL CPPP solutions (5 mg/mL). The mixture (pH = 7.0) was maintained for 2.5 h at 60 ℃, followed by keeping for 10 min in 100 ℃ water bath. The mixture was centrifuged (3000 r/min, 5 min, 4 ℃). The supernatant was precipitated overnight with anhydrous ethanol at the ratio of 1:4.5. The alcohol precipitation solution was centrifuged for 15 min at 6000 r/min (4 ℃). The solid was lyophilizedried and collected for further treatment of decolorization.

Hydrogen peroxide (H_2O_2) was used to decolorization. In summary, 1.6 mL 30 % H_2O_2 was added to 10 mL deproteinized pectin solutions (5 mg/mL). The mixture was kept in a 70 ℃ water bath for 1 h. After that, the mixture was centrifuged at 3000 r/min for 5 min at 4 ℃ and precipitated overnight with anhydrous ethanol at the ratio of 1:4. The alcohol precipitation solution was centrifuged (6000 r/min, 15 min, 4 ℃). The resulting persimmon peel pectin (PPP) was obtained after lyophilization.

2.3. Physicochemical analysis and molecular weight determination of pectin samples

2.3.1. Chemical composition

The uronic acids content was tested via sulfuric acid-carbazole colorimetry (Bitter & Muir, 1962). The Bradford method was applied to detect the protein content in pectin samples including CPPP (Bradford, 1976). Ash content was detected by carbonization and then kept in a muffle furnace (575 ℃) for 10 h and weighed after cooling in a desiccator.

The total phenolic content (TPC) was measured with Folin-Ciocalteu method with minor changes (Hosseini, Khodaiyan, Kazemi, & Najari, 2019). In brief, 1 mL of Folin-Ciocalteu reagent and 1 mL of pectin solution (1 mg/mL) were mixed and kept for 3 min. Then 5 mL of sodium carbonate solution (10 %, w/v) was added to above solution. The mixed solution was incubated for 60 min and its absorbance was measured at 765 nm. The standard curve was generated by gradient gallic acid solution (20, 40, 60, 80, 100 μg/mL). TPC in pectin sample was expressed as gallic acid equivalents (GAE) percentage (g GAE/g pectin × 100 %, GAE^P). Degree of esterification (DE) was evaluated by chemical titration (Zhang et al., 2022).

2.3.2. Monosaccharide composition

Monosaccharide composition of pectin samples were investigated according to precolumn derivatization gas chromatography (GC) method (Wang, Zhang, Wu, Xu, Wang, & Lu, 2017). Briefly, hydrolysis reaction of 10 mg pectin samples and 10 mL 2 M trifluoroacetic acid (TFA) was carried out at 120 °C for 3 h, followed by vacuum-rotary evaporation to remove excess TFA, this step was repeated for three times. Then 200 μL Na_2CO_3 (0.5 mol/L) was added to samples and held at 30 °C in water bath for 45 min. The above samples were reduced by

adding 2 mL newly prepared $NaBH_4$ (4 %) and kept for 1.5 h at room temperature. The excess $NaBH_4$ was removed via 25 % (v/v) acetic acid. The obtained mixture was applied to a cation-exchanged resin column (10 mL) eluted with 20 mL of water and the eluate was dried repeatedly with methanol for 4 times and then kept at 85 ℃ for 4 h. Then, 2 mL pyridine and 0.5 mL *n*-propylamine were added for amidation at 55 ℃ for 0.5 h, dried and then added 2 mL pyridine and 2 mL acetic anhydride for acetylation at 95 °C for 1 h. The mixture was concentrated and CH_2Cl_2 was added to a final volume of about 1.5 mL. Finally, the sample was filtered (0.45 μm pore size) for further analysis.

Monosaccharide composition was analyzed by GC (Shimadzu 2014C, Japan) connected with a DB-17 capillary column (30 m × 0.25 mm × 0.25 μm, Agilent, USA) and a flame ionization detector (FID). The chromatographic conditions were as follows: the injection volume was 1 μL; the flow rates of N_2, H_2, and air were 1.5 mL/min, 60 mL/min, and 450 mL/min, respectively; the temperatures of injector and detector were 250 °C and 280 °C, respectively; the temperature was programmed and the detection time was 45 min.

2.3.3. Molecular weight

The average molecular weight (M_w) of pectin samples were measured through a high performance gel permeation chromatography (HPGPC) combined with 2414 refractive index (Waters, USA). Briefly, 2 mg sample was fully dissolved in 1 mL mobile phase (0.2 M NaCl-20 mM PBS (pH 6.0) and filtered through 0.22 μm membrane. Then, the prepared samples was tested by TSK-Gel 5000 PWXL (7.5 mm*30 cm) at the flow rate of 0.5 mL/min with dextran standards (5.2 kDa, 11.6 kDa, 23.8 kDa, 48.6 kDa, 148 kDa, and 273 kDa) for calibration.

2.4. UV and FT-IR spectra analysis

The UV absorption features of pectin solutions (0.5 mg/mL) were measured by a UV–vis spectrophotometer (UV-2550, SHIMADZU) at the wavelength of 200–600 nm. To get the FT-IR spectra (4000–400 cm^{-1}) of pectin samples, fully dried pectin and KBr powder were ground (1:100, w/w), made into sheet sample and then detected by a FT-IR spectrometer (Bruker Vetex 70, Germany).

2.5. X-ray diffraction (XRD) analysis

X-ray diffractometer (Bruker, Germany) was applied to test the crystal properties of pectin. After the sample was fully dried, the powder diffraction method was used for determination. The scanning range was 5–50° and the step width was 0.0197° for analysis and testing.

2.6. Nuclear magnetic resonance (NMR) spectroscopy analysis

Hydrogen-1 nuclear magnetic resonance (^1H NMR) properties of pectin samples were got via avance neo 400 MHz spectrometer (Bruker, Switzerland). 50 mg of PPP or CCP were dissolved in 1 mL of D_2O and scanned 16 times to obtain the spectrum.

2.7. Micromorphology analysis

Fully dried pectin samples were loaded on the workbench fixed by tape and non-bonded samples were removed with an ear wash ball. After the gold spraying treatment, the micromorphology of PPP and CCP were observed by scanning electron microscope (S-3400N, Japan) in different visual fields at 5.0 kV.

2.8. Differential scanning calorimetric (DSC) analysis

Differential scanning calorimetry (TA Q2000, USA) was applied to detect the thermal features of PPP and CCP (Zhang, Liu, Tao, & Wei, 2016). 5 mg pectin sample was added to an aluminum crucible. N_2 flow rate was 50 mL/min and the temperature scanning range was from 40 to 300 °C at the rate of 10 °C/min.

2.9. Anti-oxidant activity analysis

2.9.1. The ability of ABTS radical scavenging

The ABTS radical scavenging determination of pectin samples was applied according to reported experimental procedure with minor changes (Re, Pellegrini, Proteggente, Pannala, Yang, & Rice-Evans, 1999). In brief, ABTS solution (7.4 mM) and potassium persulfate (2.45 mM) were mixed, kept for 16 h and diluted with PBS (pH 7.4) to ensure the absorbance (734 nm) of ABTS•+ working fluid was 0.70 ± 0.02. Then, 2 mL ABTS•+ solution was added to tubes loaded with 0.5 mL different samples (0–5 mg/mL), kept for 5 min in dark place and measured by a detector at 734 nm.

The ABTS radical scavenging rate (%) = $(1 - (A_1\text{-}A_2)/A_0) \times 100$ %. A_0: ABTS•+ + water (water instead of pectin sample); A_1: ABTS•+ + pectin sample; A_2: water + pectin sample (water instead of ABTS•+); A stands for absorbance at 734 nm.

2.9.2. The activity of DPPH radical scavenging

The pectin's scavenging capacities of DPPH• were tested according to the reported method with litter modifications (Sun et al., 2018). Briefly, 2 mL DPPH• working solution (100 μmol/L) was added to tubes added with 0.5 mL serial pectin samples (0–5 mg/mL). Then, the mixture was reacted in the dark for 30 min and its absorbance was measured at 517 nm.

The DPPH radical scavenging activity (%) = $(1 - (A_1\text{-}A_2)/A_0) \times 100$ %. A_0: DPPH• + water (water instead of pectin sample); A_1: DPPH• + pectin sample; A_2: ethanol + pectin sample (ethanol instead of DPPH•); A: absorbance.

2.10. Gut microbial community analysis

6–8-week-old male C57BL/6 mice were purchased from SJA Laboratory Animal Co. Ltd (Changsha, Hunan Province, China). The Animal Ethics Committee of Xi'an Jiaotong University approved the study protocol (Permission No. SCXK 2021-1005). The mice were housed under controlled conditions at 23 ± 2 °C, humidity at 40–60 % and 12 h light/dark cycles for free diet and drinking water. After 7 days of acclimatization, the mice were divided into two groups: Control (n = 5), PPP (200 mg/kg/day PPP, n = 5). After oral gavage of PPP or normal saline for 4 weeks, the feces of mice were collected for microbiological analysis.

The PowerSoil DNA isolation kit (Mo Bio Laboratories, Carlsbad, CA, USA) was used to extract total bacterial DNA in mice fecal samples. The hypervariable V3–V4 regions of the 16S rRNA gene were amplified by PCR with 335F primer (5′-ACTCCTACGGGAGGCAGCA-3′) and 806R primer (5′- GGACTACHVGGGTWTCTAAT-3′), and then sequenced on the Illumina HiSeq 2500 platform (Illumina Inc., San Diego, CA, USA). The obtained sequencing data in this study were further analyzed at the BMK Cloud platform (https://www.biocloud.net/). Operational taxonomic units (OTUs) were clustered with 97 % similarity by UPARSE (version 7.1) and annotated based on the SILVA database (https://www.arb-silva.de) using Ribosomal Database Project Classifier (version 2.2). The alpha diversity of gut microbiota, partial least squares discriminant analysis (PLS-DA), and sample heatmap based on binary-jaccard distance were carried out by QIIME2 (https://qiime2.org/). The biomarkers were analyzed by linear discriminant analysis coupled with effect size (LefSe, https://huttenhower.sph.harvard.edu/lefse/).

2.11. Statistical analysis

All experiments and measurements were performed at least three times. Data were presented as means ± SD. Analysis of variance (ANOVA) of quadratic model was conducted via Design Expert 8.06. The statistical differences between data were analyzed by Unpaired *t* test (*

= $p < 0.05$, ** = $p < 0.01$, *** = $p < 0.001$ and ns indicate no significance) via Graphpad Prism 8.0.1 (GraphPad Software, USA).

3. Results and discussion

3.1. Extraction results of PPP and statistical analysis

The CPPP's single factor extraction results by subcritical water were listed in Supplementary Fig. 1. With the increase of temperature and time, the CPPP yield first increased and then decreased, maximum CPPP extraction yield appeared at about 140 ℃ and 3 min (Supplementary Fig. 1A-B), respectively. The CPPP yield increased with the increase of S:W and then tended to be flat when the S:W reached between 15 and 30 (Supplementary Fig. 1C). When stirring rate increased, the CPPP yield had fewer increase compared with S:W. Thus, temperature, time and S:W ratio had high influence on the CPPP extraction yield than stirring rate in this study.

Basing on above single factor experimental results and BBD analysis, 17 independent experiments were conducted to evaluate the effect of three extraction variables, including temperature (120–160 ℃), time (1–5 min) and S:W ratio (1:5–1:15), on the extraction yield of CPPP. Supplementary Table 1 showed the specific information of BBD as well as the actual yield of each experiment. As we can see, the obtained minimum and maximum CPPP yield in this part were 2.86 % and 7.67 % from the experiment 4 (temperature of 160 ℃, extraction time of 5 min, S:W ratio of 1:10) and experiment 17 (extraction temperature was 140 ℃, extraction time was 3 min, S:W ratio was 1:10), respectively. The low yield might be attributed to the serious thermal degradation of pectin at high extraction temperature (Zhang et al., 2022). While higher yields were likely to occur around 140 ℃, the same phenomenon could also be found in process of extracting jackfruit peel pectin with subcritical water (Li et al., 2019).

After the analysis of variance (ANOVA), the analysis results were listed in Supplementary Table 2. As expected, the p-value (<0.0001) of this regression model was extremely significant and lack of fit (0.1026) in optimized model was not significant, indicating that the CPPP yield was well fitted with the resulting model. Also, the three independent variables in this study were significantly correlated with CPPP yield, R^2 of which was 0.9963. In addition, the P-values of them (X_1^2, X_1, X_2^2, X_3^2, X_1X_2 and X_2) were smaller than 0.05, revealing that all of them had significantly effects on CPPP yield (the smaller of the P value is, the stronger significant effect of the factor are). In comparison, P-values of X_3 (0.3452), X_1X_3 (0.5711) and X_2X_3 (0.4963) were bigger than 0.05, indicating that extraction yield of CPPP was not significantly affected by these factors. The obtained model about CPPP yield was listed below:

CPPP yield (%) $= 7.62 - 0.62X_1 - 0.15X_2 + 0.055X_3 - 0.24X_1X_2 + 0.045X_1X_3 + 0.055X_2X_3 - 2.87X_1^2 - 0.73X_2^2 - 0.61X_3^2$.

X_1–X_3 are corresponding independent variables (X_1 is temperature, X_2 is time, X_3 is S:W ratio).

The three-dimensional (3D) response surface plots basing on any two independent factors (temperature, time and S:W ratio) and response value (CPPP yield) were shown in Fig. 1. It was obvious that the higher CPPP yield appeared in the condition of higher extraction temperature and longer extraction time agents. However, this phenomenon no longer existed with increased of temperature or time, which may attribute to the degradation/pyrolysis of pectin under severe environment (Abid, Renard, Watrelot, Fendri, Attia, & Ayadi, 2016). Obviously, the interaction between X_1 and X_2 was the most significant, which was consistent with result in Supplementary Table 2. The predictive optimal extraction yield of CPPP by the model was 7.66 %. To verify the predicted result, the optimal conditions were conducted as follows: extraction temperature of 138 °C, extraction time of 2 min 50 s and S:W ratio of 1:10.02. The extract rate of three independent verification experiments was 7.62 ± 0.07 %, which was very close to the above predictive value (7.66 %), indicating that the regression model in this study was precise and could be used to the prediction of CPPP extraction yield (Xu, Wang, Zhuo, Ye, & Pu, 2020). The optimal extraction temperature in this study was close to apple pomace pectin (140 °C) and the same as jackfruit peel pectin

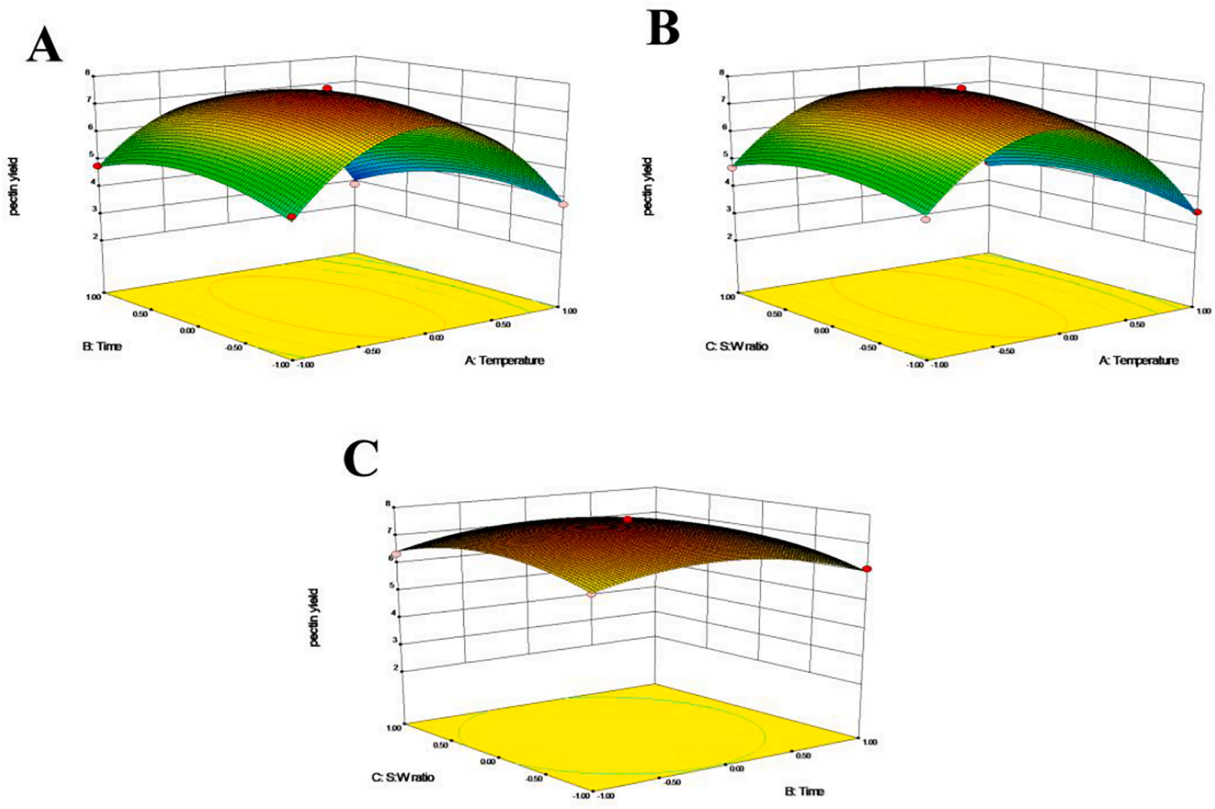

Fig. 1. Response surface (3D) plots of three variables (temperature, time and S:W) on CPPP extraction rate (%).

(138 °C). However, the extraction time and S:W were lower than both of them. In addition, the influence of three factors on the extraction yield was temperature > time > S:W ratio or liquid/solid (Li et al., 2019; Wang & Lu, 2014), which was consistent with this study. To sum up, those above results revealed that the extraction temperature may be similar in some pectin extraction from fruit peel or waste by the subcritical water extraction technology.

In order to improve the content of total sugar and quality of obtained pectin and reduce effect on biological activity produced by other non-sugar substance, papain and H_2O_2 were used for deproteinization and decolorization, respectively. After treatment of deproteinization and decolorization, the protein content decreased from 11.90 ± 0.21 % to 2.00 ± 0.14 % and 78.56 % of the colour in CPPP was removed (data not shown), indicating the effectiveness of deproteinization and decolorization.

3.2. Physicochemical composition and molecular weight determination

PPP was obtained following method in 2.2 in this part. The uronic acids content of PPP (64.03 ± 0.82 %) was lower than that of CCP (73.40 ± 0.60 %), CPPP (67.14 ± 0.67 %, data not shown) and PPP (71.39 ± 0.32 GalA%) obtained by hot citric acid (pH 2.0) (Jiang et al., 2020). Interestingly, when other extraction conditions were certain, the uronic acids in pectic polysaccharides extracted from apple pomace by SCW decreased with the increasing temperature (Zhang et al., 2022). In addition, jackfruit peel pectin extracted by SCW (JFP-S) was lower that had more hairy regions and side chains and lower content of GalA than jackfruit peel pectin extracted by traditional citric acid (JFP-C) (Li, Fan, Wu, Jiang, & Shi, 2019). So, the low uronic acids content of PPP may be the result of thermal degradation of some pectins as well as retain of more hairy regions and side chains in the process of SCW extraction instead of a consequence of the use of H_2O_2 during the decolorization treatment. The DE of PPP (40.61 ± 0.03 %) was higher ($p < 0.05$) than CCP (26.63 ± 0.04 %) and lower than that of pectin (68.37 ± 2.78 %) from sour cherry pomace extracted by the microwave-assisted extraction method (Hosseini, Parastouei, & Khodaiyan, 2020).

According to TPC results in Table 1, the TPC of PPP and CCP were 1.53 ± 0.01 % GAE^P and 0.02 ± 0.17 % GAE^P, respectively. However, TPC of PPP was lower than pectin extracted by microwave from pistachio green hull (0.18 % GAE^P) and pectin extracted from sour orange peel by ultrasound assisted method (0.340 ± 0.03 % GAE^P) (Hosseini et al., 2019).

The monosaccharide composition of PPP and CCP was shown in Table 1. The PPP consisted of Rha, Ara, Xyl, Man, Glu, Gal, GluA, and GalA at a molar ratio of 2.52:15.88:11.46:3.18:8.90:9.74:1.52:46.80, respectively, indicating that the PPP was a hetero-polysaccharide. Man and GluA were not found in CCP. The molar ratio of Rha in PPP was 3.32 times that of CCP (4.76 ± 0.04 %). The contents of Xyl had no significant difference between PPP and CCP. Compared with CPP, arabinose and glucose in PPP were significantly higher than those in CCP, while Gal and GalA were significantly lower than that in CCP. In general, PPP was a kind of typical pectic polysaccharides.

HPGPC was applied to determination of average molecular weight (M_w) of pectin samples. The M_w of PPP was 21.79 kDa, which was smaller than CCP (M_w = 941.56 kDa) and CPPP (M_w = 29.84 kDa), indicating the low M_w of PPP was not a consequence of decolorization and deproteinization in this study. Interestingly, the M_w of PPP in this study was also smaller than that of PPP (228 kDa, 328 kDa, respectively) obtained by hot acid in previous reports (Jiang et al., 2020; Munoz-Almagro et al., 2021). When the extraction time was same, the M_w of pectic polysaccharides extracted from apple pomace will decrease with the increase of extraction temperature; when the extraction temperature was identical, the M_w of pectic polysaccharides extracted from apple pomace will decrease with the increase of extraction time (Zhang et al., 2022). So, the low M_w of PPP may be related to degradation of glycosidic bond under high temperature compared with other extraction methods.

Table 1
Physicochemical composition, degrees of esterification and molecular weight of PPP and CCP.

	PPP	CCP
Physicochemical indexes		
Uronic acids (%)	64.03 ± 0.82^a	73.40 ± 0.60^b
Protein content (%)	2.00 ± 0.14^a	2.31 ± 0.09^b
Total phenolic content (% GAE^P)	1.53 ± 0.01^a	0.02 ± 0.17^b
Ash content (%)	2.11 ± 0.05^a	2.79 ± 0.01^b
DE (%)	40.61 ± 0.03^a	26.63 ± 0.04^b
Monosaccharide composition (mole ratio/%)		
Rhamnose	2.52 ± 0.02^a	2.83 ± 0.03^b
Arabinose	15.88 ± 0.04^a	4.76 ± 0.04^b
Xylose	11.46 ± 0.03^a	11.56 ± 0.04^a
Mannose	3.18 ± 0.03	–
Glucose	8.90 ± 0.07^a	7.22 ± 0.04^b
Galactose	9.74 ± 0.08^a	12.67 ± 0.03^b
Glucuronic acid	1.52 ± 0.03	–
Galacturonic acid	46.80 ± 0.05^a	60.97 ± 0.12^b
Molecular weight (kDa)	21.79 ± 0.23^a	941.56 ± 7.68^b

Note: PPP: Persimmon peel pectin; CCP: Commercial citrus pectin; DE: Degree of esterification; -: Not detected; GAE^P: Gallic acid equivalents (GAE) percentage per g test sample (g GAE/g sample × 100 %); Monosaccharide composition is determined by gas chromatography; Averages with different superscript letters in the same line (a–b) represent there is significant difference between the pectin samples ($p < 0.05$) in Unpaired *t* test.

3.3. UV and FTIR analysis

The UV scanning spectra of PPP and CCP at the range of 200 to 600 nm was obtained in Fig. 2A. There was no sensible absorption peak at 260 nm, indicating that nucleic acid was absent in CCP and PPP. The absorption at 280 nm in PPP and CCP was obverted. To sum up, PPP had fewer protein content compared with CCP.

The test infrared spectra (IR) were shown in Fig. 2B. It was clear that the IR spectrum of PPP was almost the same as CCP due to their similar chemical composition. The hydroxyl absorption peak appeared at 3422 cm^{-1}, the stretching vibration signal of C—H located at 2921 cm^{-1}, and the variable angle vibration absorption signal of C—H appeared at 1420 cm^{-1}. The strong characteristic absorption signal at 1735 cm^{-1} was the absorption peak of the esterified carboxyl group (C═O), and the signal of 1604 cm^{-1} was C═O asymmetrical stretching vibration of free carboxyl group (Wang et al., 2015), indicating that PPP contained galacturonic acid. Furthermore, it was difficult to identify the IR characteristics (1300–800 cm^{-1}) of monosaccharide composition of pectin attributed to spectrum overlap (Mohnen, 2008). Hence, the characteristics of PPP need to be further investigated combining with other analytical methods, such as smith degradation, methylation, and NMR etc.

3.4. Micromorphology analysis

SEM was applied to observe the microstructure of PPP and CCP in this study. The micromorphology of them was shown in Fig. 2C and D. Specifically, PPP exhibited massive accumulation of polysaccharide particles with rough surface in irregular forms. CCP had a more compact surface compared with PPP. The rough surface and small particles may endow PPP with good solubility because of its higher surface area. The difference in microstructure between CCP and PPP might be attributed to their difference in chemical compositions (Jiang et al., 2020), M_w as well as randomness of flocculation during drying.

3.5. XRD analysis

The amorphous samples were universally reported with a broad peak while the crystalline sample indicates several sharp signals in these

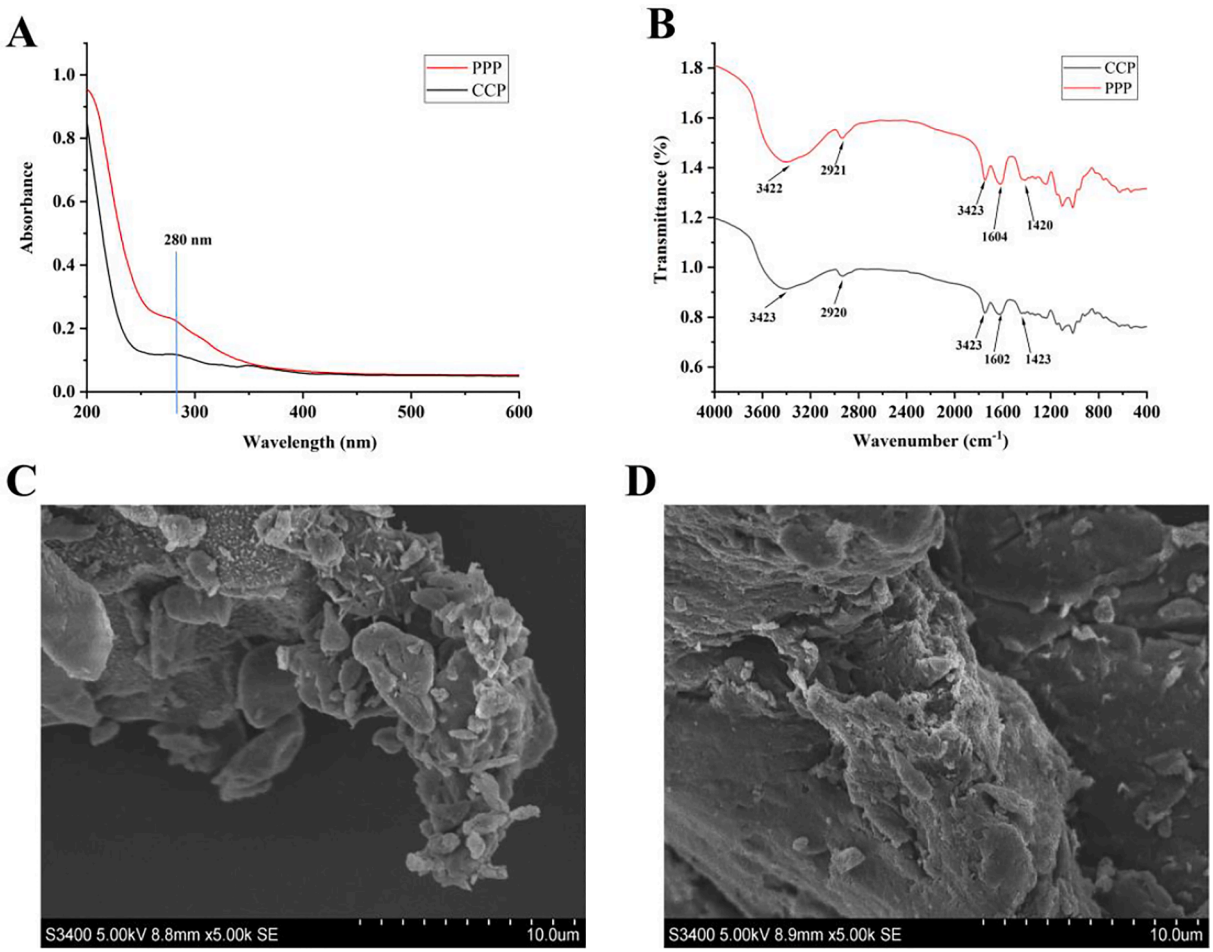

Fig. 2. The UV spectra (A) and FTIR spectrum (B) of persimmon peel pectin (PPP) and commercial citrus pectin (CCP); Surface microscopic images of persimmon peel pectin (PPP) (C) and commercial citrus pectin (CCP) (D).

patterns. The XRD analysis of PPP and CCP were shown in Fig. 3A. Both of them had obvious peak at 21°, which was crystalline nature of pectin samples (Jiang, Du, Zhang, & Li, 2018). An amorphous nature (from 11° to 20°) was observed in CCP, which was consistent with the result of pectin obtained from *Garcinia mangostana* L. rind (Wathoni et al., 2019). While PPP showed similar crystal peaks with the persimmon peel pectin extracted using hot citric acid (Jiang et al., 2020). The difference of diffraction peaks between CCP and PPP may be explained by different chemical compositions and source of raw materials.

3.6. ^{1}H NMR spectrum analysis

The analysis of ^{1}H NMR was conducted in order to observe structural features of PPP. As was shown in Fig. 3B, the representative chemical shifts of polysaccharides were observed at δ_H 3.0 to 5.5 and the peak appearing at δ_H 4.79 was the signal of D_2O. Clearly, the chemical shift of esterified GalA units (–OCH_3) was observed at 3.80 ppm (Zhang, He, Cheng, Xu, Cheng, & Wu, 2021). According to the previous study, the signals at 4.0 to 5.0 ppm and 5.0 to 5.6 ppm revealed the existence of β-glycosidical and α-glycosidical in this two pectin samples, respectively (Yang, Nisar, Hou, Gou, Sun, & Guo, 2018). The chemical shifts of H-1, H-2, H-3, and H-4 of GalA and methyl GalA units were observed at 5.09/4.96, 3.77/3.72, 4.02/4.00 and 4.40/4.47 ppm, respectively. The H-5 of free GalA units around in 4.76 ppm may be overlapped with solvent peak. In addition, the signals at around 2.10 ppm in PPP may be due to existence of acetyl groups, which was similar to that of *Cerasus humilis* pectic polysaccharides enriched in RG-I (Zhang et al., 2021). The chemical shifts at 1.27 ppm revealed the existence of Rha, which was consistent with the data of monosaccharide composition.

3.7. Thermal analysis

DSC was applied to explore the thermodynamic features of pectin samples to minor the structural and functional group differences between pectin samples (Jiang et al., 2020; Wang & Lu, 2014). Two endothermic peaks as well as one exothermic peak were observed in the DSC curves (Fig. 3C). The first endothermic peaks of CCP and PPP were 159.38 ℃ and 165.64 ℃, respectively. Compared with CCP, the relatively higher endothermic peak represented stronger water holding capacity in PPP (Zhang et al., 2016). The second endothermic peaks of CCP and PPP were 217.06 ℃ and 197.08 ℃, respectively, indicating the melting of pectin samples. The maximum exothermic peaks for CCP and PPP were observed at 237.69 ℃ and 228.05 ℃, respectively, representing the degradation of pectin samples. The results suggested that PPP possessed good thermal stability as CCP, which was crucial for its potential application in food industry, such as bread, cakes and pastrie (Combo et al., 2013). Moreover, PPP owned a wider exothermic peak, which might be attributed to its decentralized M_w distribution and abundant monosaccharide composition.

3.8. Antioxidant activities of PPP in vitro

3.8.1. ABTS radical scavenging capacity

The scavenging activity to ABTS radical was a method to evaluate antioxidant capacity of polysaccharides. Fig. 4A described the reduction ability of CCP, PPP and Vc at different tested concentrations. With

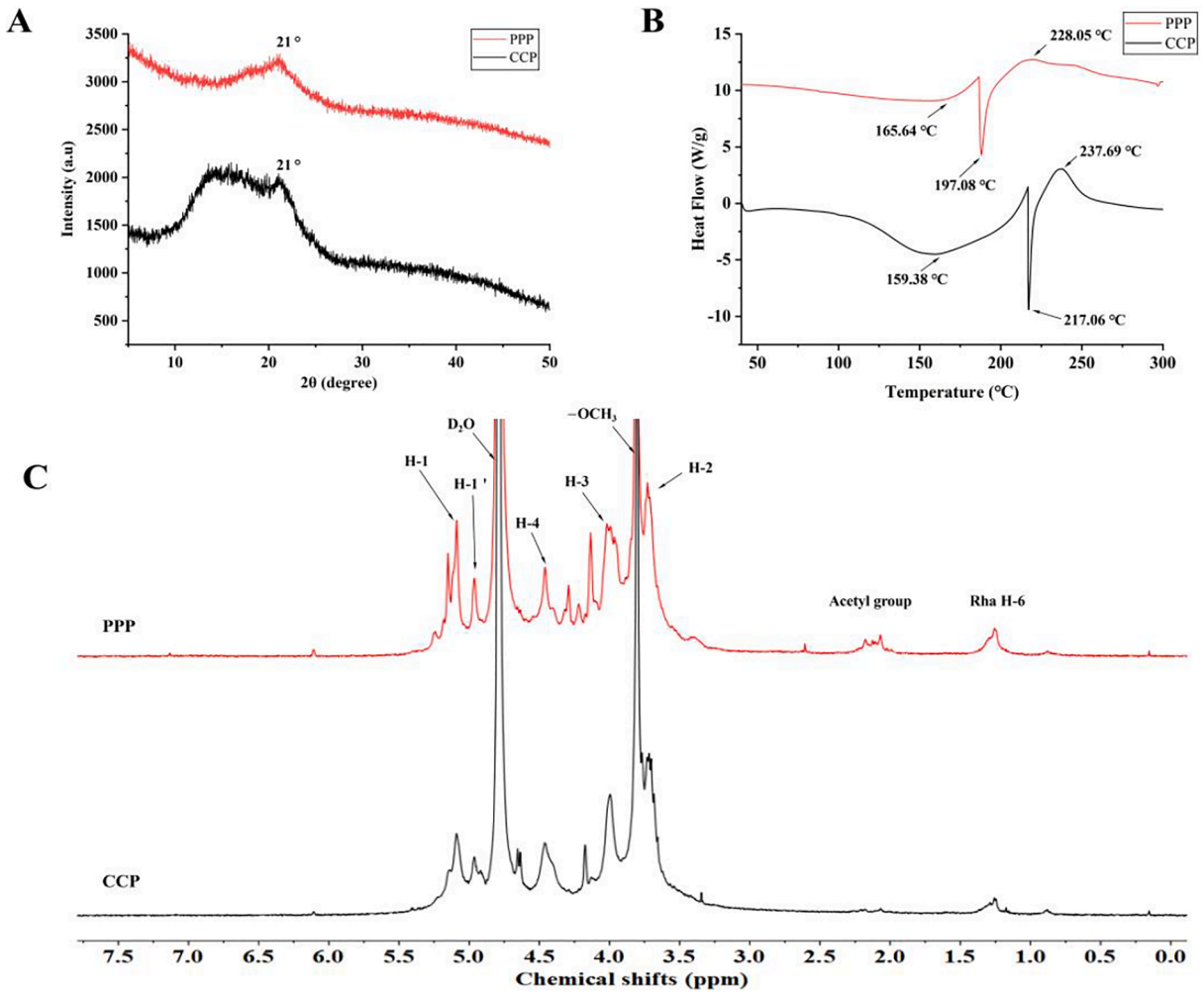

Fig. 3. XRD diffractogram (A), The ^{1}H NMR spectrum (B), Thermal analyses of differential scanning calorimetric curves (C) of persimmon peel pectin (PPP) and commercial citrus pectin (CCP).

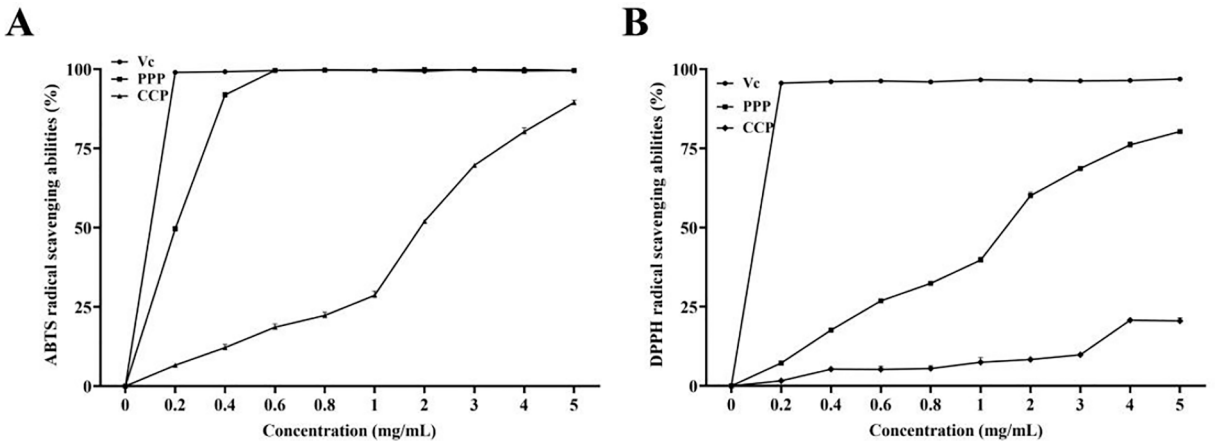

Fig. 4. ABTS (A) and DPPH (B) radical scavenging activities in vitro of persimmon peel pectin (PPP) and commercial citrus pectin (CCP). Note: Vc: Vitamin C.

increase in PPP concentration up to 0.6 mg/mL, the antioxidant activity was increased with a steep slope. Then the antioxidant activity of PPP entered in plateau and was close to antioxidant activity of Vc. CCP also showed strong scavenging activity to ABTS•+ and its observed highest level was 89.47 % at 5 mg/mL. The IC_{50} values of the PPP and CCP were 0.21 mg/mL and 2.06 mg/mL according to ABTS assay, indicating that the ABTS scavenging radical activity of the PPP was approximate 9.8-fold higher than CCP.

3.8.2. *DPPH radical scavenging activity*

The radical scavenging capacities of CCP and PPP to DPPH• were shown in Fig. 4B, both of them were increased with the increase of

pectin's concentration (0–5 mg/mL). The scavenging capacity of CCP, PPP and Vc reached up to 20.50 %, 80.32 % and 96.88 % at 5 mg/mL, respectively. The IC_{50} of the PPP was 1.46 mg/mL according to DPPH• scavenging assay, which was higher than sour orange peel pectin at the concentration of 5 mg/mL (Hosseini et al., 2019). The difference in antioxidant activity in vitro between PPP and CCP might be attributed to their differences in raw materials, M_w and TPC contents.

3.9. The effects of PPP on the composition of the gut microbiota

The effects of PPP on composition of the gut microbiota in mice was investigated by 16S rRNA high throughput sequencing. The results of Rarefaction and Shannon curves in Supplementary Fig. 2A and B revealed that the majority of bacterial diversity in all tested samples had been captured. The ACE and Chao1 index in PPP group were significantly higher than that of Control group (Fig. 5A and B), while the Simpson and Shannon index had no significant differences between PPP and Control group (Supplementary Fig. 2C and D). With regard to beta-diversity (Fig. 5C and D), PLS-DA and sample heatmap based on binary-jaccard clearly revealed that an apparent clustering separation occurred between the PPP and Control group, indicating that the microbial composition was elevated by PPP.

As was shown in Fig. 5E, both PPP and Control group mainly consisted of Bacteroidota, Firmicutes, Verrucomicrobiota and

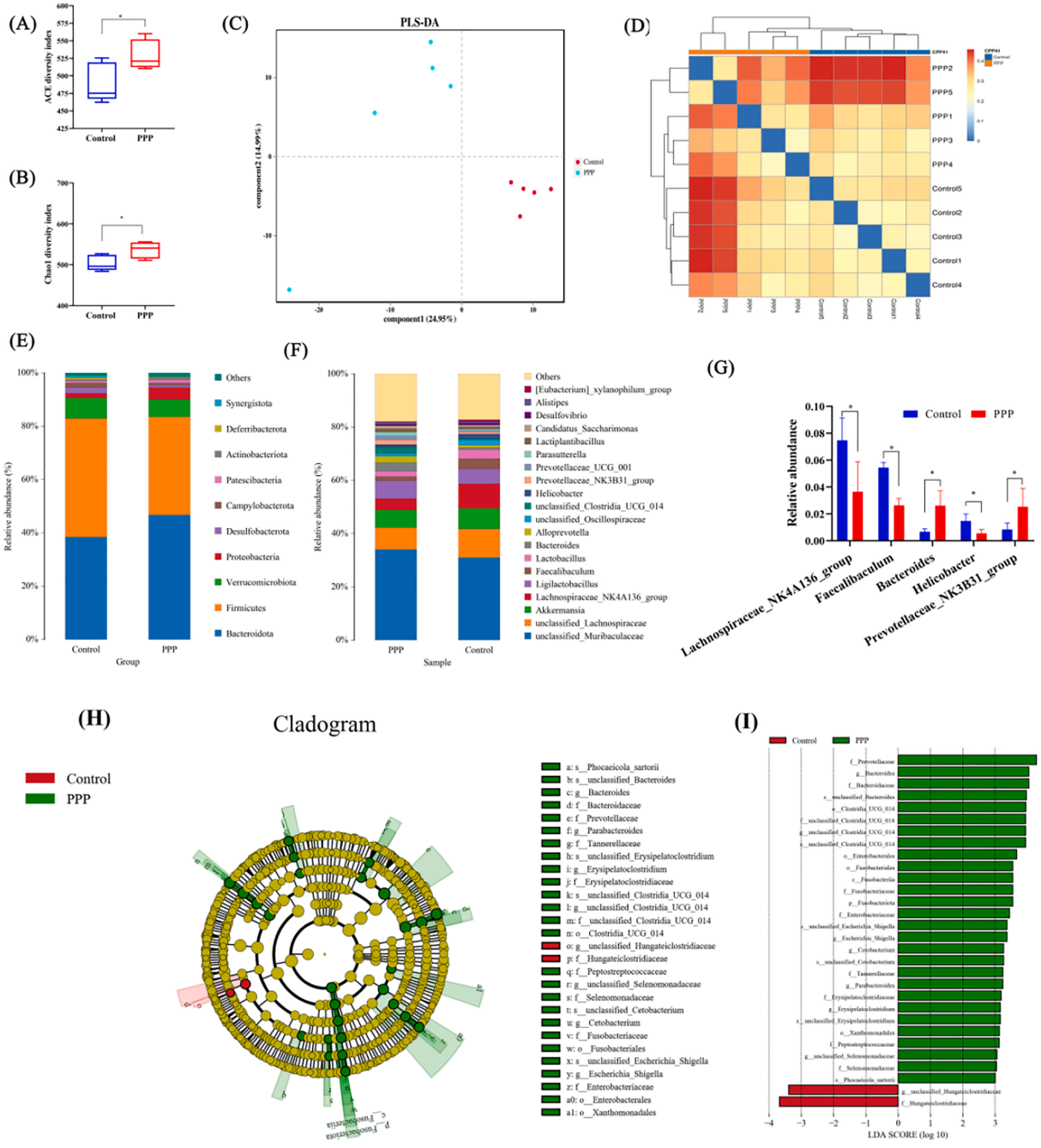

Fig. 5. Effect of PPP on gut microbiota. α-diversity of ACE (A) and Chao1 (B) indexes; PLS-DA plot (C); sample heatmap based on binary-jaccard (D); relative abundance at phylum level (E); relative abundance at genes level (F); The relative abundance of some bacterial at genus level with significant differences between PPP and Control groups (G); Cladogram (H) LDA scores (I) of the corresponding bacteria taxa (LDA scores of >3.0). Data in A and B are showed as mean ± SD, significance = * indicate $p < 0.05$.

Proteobacteria at the phylum level, and the relative abundance of them were >92.4 % of microbes. Interestingly, there was no significant change in the relative abundance at phylum level (data not shown). In the genus-level analysis, 4 of the top 20 genera in relative abundance showed significant differences between PPP and Control group (Fig. 5F and G). When compared to Control group, *Bacteroides* and *Prevotellaceae* NK3B31 group were significantly increased in PPP group, which was similar to results of mulberry fruit polysaccharides (Chun et al., 2018) and *Lycium barbarum* polysaccharides (Yu et al., 2019), while *Lachnospiraceae* NK4A136 group, *Faecalibaculum* and *Helicobacter* were significantly decreased in PPP group ($p < 0.05$). The decrease of *Helicobacter* was in accordance with the study of *Artemisia sphaerocephala* Krasch polysaccharide in diet-induced obese mice (Junjun, Han, Ximei, Dongyan, Xinzhong, & Junling, 2021). These results revealed that PPP could regulate structural of gut microbiota in mice.

Furthermore, the LefSe analysis was applied to identify the significantly different phylotypes in PPP and Control group. As shown in Fig. 5H and 5I, a total of 2 and 28 significant differences of specific bacterial taxa (ASVs) were enriched in Control and PPP groups (LDA score > 3), respectively. Unclassified *Hungateiclostridiaceae* was enriched in Control group at genus level, while PPP group was enriched in *Bacteroides*, *Cetobacterium*, *Erysipelatoclostridium*, *Escherichia Shigella*, *Parabacteroides*, unclassified *Clostridia* UCG 014, unclassified *Selenomonadaceae* at the at genus level, *Phocaeicola sartorii*, unclassified *Bacteroides*, unclassified *Cetobacterium*, unclassified *Clostridia* UCG 014, unclassified *Erysipelatoclostridium*, unclassified *Escherichia Shigella* at species level. After Agrocybe cylindracea polysaccharides treatment, *Bacteroides* and *Parabacteroides* were enriched in high-fat diet (HFD)-induced obese mice (Zhenjun et al., 2022). *Cetobacterium* was reported as a kind of short-chain fatty acids producing bacteria (Jun-Yan et al., 2022). E*rysipelatoclostridium* was reported significantly higher in the High-Fat Diet (HPD) group in mice than in the control group (Jae-Kwon et al., 2021). In addition, *Clostridia* was identified as the phenotypic biomarker of the *Cyclocarya paliurus* polysaccharide group (200 mg/kg body weight) compared with control group (Ting et al., 2021). The enrichment of *Phocaeicola sartorii* was agreement with the study of Saccharina japonica fucan in high fat diet-induced obesity (Bin et al., 2022). Overall, these above results revealed that PPP selectively enriched some bacteria taxa in mice and might have anti-obesity activity.

4. Conclusions

In this work, the optimal extraction conditions of CPPP were obtained via subcritical water. 83.19 % protein and 78.56 % of the colour in CPPP was removed after the treatment of deproteinization and decolorization. The resulting PPP had relatively low M_w of 21.79 kDa and it mainly contained GalA, Ara, Xyl, Gal, and Glu at the ratio of 46.80: 15.88: 11.4: 9.74: 8.90. PPP might be applied to food or pharmaceutical industry due to its relatively good thermal stability, in vitro antioxidant activity and prebiotic properties in regulation of gut microbiota in mice. This study would provide a new method for PPP extraction and theoretical basis for further studying regarding structural features, biological activities as well as commercial exploitation of persimmon peel. However, the fine structure and structure–function relationships of PPP need to be further investigated in further research.

CRediT authorship contribution statement

Yanlong Cui: Investigation, Methodology, Formal analysis, Data curation, Writing – original draft, Writing – review & editing. **Shuang Wang:** Investigation, Data curation, Visualization, Writing – review & editing. **Shuxuan Wang:** Software, Investigation, Data curation. **Siyue Cao:** Data curation. **Xin Wang:** Methodology, Formal analysis, Investigation, Funding acquisition. **Xin Lü:** Conceptualization, Supervision, Funding acquisition, Resources, Writing – review & editing.

Declaration of Competing Interest

The authors declare that they have no known competing financial interests or personal relationships that could have appeared to influence the work reported in this paper.

Data availability

No data was used for the research described in the article.

Acknowledgements

This work is supported by the key-point research and invention program of Shannxi province (NO. 2021ZDLNY05-06), Chinese Universities Scientific Fund (NO. 2452018062), and National Natural Science Foundation of China (Grant No. 32001652).

Appendix A. Supplementary data

Supplementary data to this article can be found online at https://doi.org/10.1016/j.fochx.2022.100486.

References

Abid, M., Renard, C. M. G. C., Watrelot, A. A., Fendri, I., Attia, H., & Ayadi, M. A. (2016). Yield and composition of pectin extracted from Tunisian pomegranate peel. *International Journal of Biological Macromolecules, 93*, 186–194. https://doi.org/10.1016/j.ijbiomac.2016.08.033

Basak, S., & Annapure, U. S. (2022). The potential of subcritical water as a "green" method for the extraction and modification of pectin: A critical review. *Food research international (Ottawa, Ont.), 161*, 111849-111849.

Bin, W., Bo, Z., Ao-Qi, D., Zhen-Yi, Z., Dong-Ze, L., Zhong-Hui, Z., … Hong, W. (2022). Saccharina japonica fucan suppresses high fat diet-induced obesity and enriches fucoidan-degrading gut bacteria. *Carbohydrate Polymers*. https://doi.org/10.1016/j.carbpol.2022.119411

Bitter, T., & Muir, H. M. J. A. B. (1962). A modified uronic acid carbazole reaction. *4*, 330-334.

Bradford, M. M. (1976). A rapid and sensitive method for the quantitation of microgram quantities of protein utilizing the principle of protein-dye binding. *Analytical Biochemistry, 72*, 248–254. https://doi.org/10.1016/0003-2697(76)90527-3

Chun, C., Li-Jun, Y., Qiang, H., Xiong, F., Bin, Z., Rui-Hai, L., & Chao, L. (2018). Modulation of gut microbiota by mulberry fruit polysaccharide treatment of obese diabetic db/db mice. *Food & Function*. https://doi.org/10.1039/c7fo01346a

Combo, A. M. M., Aguedo, M., Quievy, N., Danthine, S., Goffin, D., Jacquet, N., … Paquot, M. (2013). Characterization of sugar beet pectic-derived oligosaccharides obtained by enzymatic hydrolysis. *International Journal of Biological Macromolecules, 52*, 148–156. https://doi.org/10.1016/j.ijbiomac.2012.09.006

Das, I., & Arora, A. (2021). Kinetics and mechanistic models of solid-liquid extraction of pectin using advance green techniques- a review. *Food Hydrocolloids, 120*. https://doi.org/10.1016/j.foodhyd.2021.106931

Hamauzu, Y., & Suwannachot, J. (2019). Non-extractable polyphenols and in vitro bile acid-binding capacity of dried persimmon (Diospyros kaki) fruit. *Food Chemistry, 293*, 127–133. https://doi.org/10.1016/j.foodchem.2019.04.092

Hosseini, S., Parastouei, K., & Khodaiyan, F. (2020). Simultaneous extraction optimization and characterization of pectin and phenolics from sour cherry pomace. *International Journal of Biological Macromolecules, 158*, 911–921. https://doi.org/10.1016/j.ijbiomac.2020.04.241

Hosseini, S. S., Khodaiyan, F., Kazemi, M., & Najari, Z. (2019). Optimization and characterization of pectin extracted from sour orange peel by ultrasound assisted method. *International Journal of Biological Macromolecules, 125*, 621–629. https://doi.org/10.1016/j.ijbiomac.2018.12.096

Jae-Kwon, J., Seung-Ho, S., Seong-Eun, P., Hyun-Woo, K., Eun-Ju, K., Jeong-Sang, K., … Hong-Seok, S. (2021). Gut microbiome and metabolome profiles associated with high-fat diet in mice. *Metabolites*. https://doi.org/10.3390/metabo11080482

Jiang, Y., Du, J., Zhang, L., & Li, W. (2018). Properties of pectin extracted from fermented and steeped hawthorn wine pomace: A comparison. *Carbohydrate Polymers, 197*, 174–182. https://doi.org/10.1016/j.carbpol.2018.06.001

Jiang, Y., Xu, Y., Li, F., Li, D., & Huang, Q. (2020). Pectin extracted from persimmon peel: A physicochemical characterization and emulsifying properties evaluation. *Food Hydrocolloids, 101*. https://doi.org/10.1016/j.foodhyd.2019.105561

Jun-Yan, X., Yan-Yu, C., Jin-Xin, H., Ping, K., Zehua, L., Deli, W., … Qiuhong, X. (2022). Litchi chinensis seed prevents obesity and modulates the gut microbiota and mycobiota compositions in high-fat diet-induced obese zebrafish. *Food & Function*. https://doi.org/10.1039/d1fo03991a

Junjun, L., Han, J., Ximei, Y., Dongyan, S., Xinzhong, H., & Junling, S. (2021). The anti-obesity effects exerted by different fractions of Artemisia sphaerocephala Krasch polysaccharide in diet-induced obese mice. *International Journal of Biological Macromolecules*. https://doi.org/10.1016/j.ijbiomac.2021.04.070

Khan, I., Huang, G. X., Li, X. A., Liao, W. L., Leong, W. K., Xia, W. R., … Hsiao, W. L. W. (2019). Mushroom polysaccharides and jiaogulan saponins exert cancer preventive effects by shaping the gut microbiota and microenvironment in Apc(Min/+) mice. *Pharmacological Research, 148*. https://doi.org/10.1016/j.phrs.2019.104448

Li, W. J., Fan, Z. G., Wu, Y. Y., Jiang, Z. G., & Shi, R. C. (2019). Eco-friendly extraction and physicochemical properties of pectin from jackfruit peel waste with subcritical water. *Journal of the Science of Food and Agriculture, 99*, 5283–5292. https://doi.org/10.1002/jsfa.9729

Liu, Z., Yao, L., & Fan, C. (2015). Optimization of fermentation conditions of pectin production from Aspergillus terreus and its partial characterization. *Carbohydrate Polymers, 134*, 627–634. https://doi.org/10.1016/j.carbpol.2015.08.032

Mohnen, D. (2008). Pectin structure and biosynthesis. *Current Opinion in Plant Biology, 11*, 266–277. https://doi.org/10.1016/j.pbi.2008.03.006

Munoz-Almagro, N., Vendrell-Calatayud, M., Mendez-Albinana, P., Moreno, R., Cano, M. P., & Villamiel, M. (2021). Extraction optimization and structural characterization of pectin from persimmon fruit (Diospyros kaki Thunb. var. Rojo brillante). *Carbohydrate Polymers, 272*, 118411-118411. https://doi.org/10.1016/j.carbpol.2021.118411.

Re, R., Pellegrini, N., Proteggente, A., Pannala, A., Yang, M., & Rice-Evans, C. (1999). Antioxidant activity applying an improved ABTS radical cation decolorization assay. *Free Radical Biology and Medicine, 26*, 1231–1237. https://doi.org/10.1016/s0891-5849(98)00315-3

Si-Yuan, L., Yang, L., Shijie, T., Wancong, Z., Qiuyong, Y., Changqi, S., & Kit-Leong, C. (2021). Gracilaria lemaneiformis polysaccharides alleviate colitis by modulating the gut microbiota and intestinal barrier in mice. *Food Chemistry: X*. https://doi.org/10.1016/j.fochx.2021.100197

Smrke, T., Persic, M., Veberic, R., Sircelj, H., & Jakopic, J. (2019). Influence of reflective foil on persimmon (Diospyros kakiThunb.) fruit peel colour and selected bioactive compounds. *Scientific Reports, 9*. https://doi.org/10.1038/s41598-019-55735-1

Sun, J., Zhou, B., Tang, C., Gou, Y. R., Chen, H., Wang, Y., … Zhang, N. F. (2018). Characterization, antioxidant activity and hepatoprotective effect of purple sweetpotato polysaccharides. *International Journal of Biological Macromolecules, 115*, 69–76. https://doi.org/10.1016/j.ijbiomac.2018.04.033

Ting, W., Mingyue, S., Qiang, Y., Yi, C., Xianxiang, C., Jun, Y., … Jianhua, X. (2021). Cyclocarya paliurus polysaccharide improves metabolic function of gut microbiota by regulating short-chain fatty acids and gut microbiota composition. *Food Research International*. https://doi.org/10.1016/j.foodres.2021.110119

Ueno, H., Tanaka, M., Hosino, M., Sasaki, M., & Goto, M. (2008). Extraction of valuable compounds from the flavedo of Citrus junos using subcritical water. *Separation and Purification Technology, 62*, 513–516. https://doi.org/10.1016/j.seppur.2008.03.004

Wang, W. J., Ma, X. B., Xu, Y. T., Cao, Y. Q., Jiang, Z. M., Ding, T., … Liu, D. H. (2015). Ultrasound-assisted heating extraction of pectin from grapefruit peel: Optimization and comparison with the conventional method. *Food Chemistry, 178*, 106–114. https://doi.org/10.1016/j.foodchem.2015.01.080

Wang, X., & Lu, X. (2014). Characterization of pectic polysaccharides extracted from apple pomace by hot-compressed water. *Carbohydrate Polymers, 102*, 174–184. https://doi.org/10.1016/j.carbpol.2013.11.012

Wang, X., Zhang, L., Wu, J., Xu, W., Wang, X., & Lu, X. (2017). Improvement of simultaneous determination of neutral monosaccharides and uronic acids by gas chromatography. *Food Chemistry, 220*, 198–207. https://doi.org/10.1016/j.foodchem.2016.10.008

Wathoni, N., Yuan Shan, C., Yi Shan, W., Rostinawati, T., Indradi, R. B., Pratiwi, R., & Muchtaridi, M. (2019). Characterization and antioxidant activity of pectin from Indonesian mangosteen (Garcinia mangostana L.) rind. *Heliyon, 5*, e02299-e02299. https://doi.org/10.1016/j.heliyon.2019.e02299.

Wu, T.-R., Lin, C.-S., Chang, C.-J., Lin, T.-L., Martel, J., Ko, Y.-F., … Lai, H.-C. (2019). Gut commensal Parabacteroides goldsteinii plays a predominant role in the anti-obesity effects of polysaccharides isolated from Hirsutella sinensis. *Gut, 68*, 248–262. https://doi.org/10.1136/gutjnl-2017-315458

Xu, D. P., Wang, C. X., Zhuo, Z. H., Ye, M., & Pu, B. (2020). Extraction, purification and antioxidant activity of polysaccharide from cold pressed oil cake of 'Tengjiao' seed. *International Journal of Biological Macromolecules, 163*, 508–518. https://doi.org/10.1016/j.ijbiomac.2020.06.207

Yang, X., Nisar, T., Hou, Y., Gou, X., Sun, L., & Guo, Y. (2018). Pomegranate peel pectin can be used as an effective emulsifier. *Food Hydrocolloids, 85*, 30–38. https://doi.org/10.1016/j.foodhyd.2018.06.042

Yoo, D. I., & Shin, Y. (2020). Application of persimmon (Diospyros kaki L.) peel extract in indigo dyeing as an eco-friendly alternative reductant. *Fashion and Textiles, 7*. https://doi.org/10.1186/s40691-020-00215-8

Yu, D., Yamei, Y., Dan, C., Linwu, R., Jia, M., Lu, L., … Youlong, C. (2019). Modulating effects of polysaccharides from the fruits of Lycium barbarum on the immune response and gut microbiota in cyclophosphamide-treated mice. *Food & Function*. https://doi.org/10.1039/c9fo00638a

Zhang, F., Zhang, L. S., Chen, J. X., Du, X. Y., Lu, Z. M., Wang, X. Y., … Lu, X. (2022). Systematic evaluation of a series of pectic polysaccharides extracted from apple pomace by regulation of subcritical water conditions. *Food Chemistry, 368*. https://doi.org/10.1016/j.foodchem.2021.130833

Zhang, S. K., He, Z. Y., Cheng, Y., Xu, F. Z., Cheng, X. X., & Wu, P. (2021). Physicochemical characterization and emulsifying properties evaluation of RG-I enriched pectic polysaccharides from Cerasus humilis. *Carbohydrate Polymers, 260*. https://doi.org/10.1016/j.carbpol.2021.117824

Zhang, Z. H., Liu, Z. Q., Tao, X. Y., & Wei, H. (2016). Characterization and sulfated modification of an exopolysaccharide from Lactobacillus plantarum ZDY2013 and its biological activities. *Carbohydrate Polymers, 153*, 25–33. https://doi.org/10.1016/j.carbpol.2016.07.084

Zhenjun, Z., Rui, H., Aohuan, H., Juan, W., Wei, L., Shujian, W., … Yu, D. (2022). Polysaccharide from Agrocybe cylindracea prevents diet-induced obesity through inhibiting inflammation mediated by gut microbiota and associated metabolites. *International Journal of Biological Macromolecules*. https://doi.org/10.1016/j.ijbiomac.2022.04.107